Bundle Sheath Leakiness and Light Limitation during C_4 Leaf and Canopy CO_2 Uptake[1][W][OA]

Johannes Kromdijk*, Hans E. Schepers, Fabrizio Albanito, Nuala Fitton, Faye Carroll, Michael B. Jones, John Finnan, Gary J. Lanigan, and Howard Griffiths

Physiological Ecology Group, Department of Plant Sciences, University of Cambridge, Cambridge CB2 3EA, United Kingdom (J.K., H.G.); Biobased Products, Agrotechnology and Food Science Group, Wageningen University and Research Center, 6708 PD Wageningen, The Netherlands (H.E.S.); Botany Department, School of Natural Sciences, Trinity College Dublin, Dublin 2, Ireland (F.A., N.F., F.C., M.B.J.); Teagasc, Oak Park Crops Research Centre, Carlow, Ireland (J.F.); and Teagasc, Johnstown Castle Environmental Research Centre, Wexford, Ireland (G.J.L.)

Perennial species with the C_4 pathway hold promise for biomass-based energy sources. We have explored the extent that CO_2 uptake of such species may be limited by light in a temperate climate. One energetic cost of the C_4 pathway is the leakiness (ϕ) of bundle sheath tissues, whereby a variable proportion of the CO_2, concentrated in bundle sheath cells, retrodiffuses back to the mesophyll. In this study, we scale ϕ from leaf to canopy level of a *Miscanthus* crop (*Miscanthus* × *giganteus* hybrid) under field conditions and model the likely limitations to CO_2 fixation. At the leaf level, measurements of photosynthesis coupled to online carbon isotope discrimination showed that leaves within a 3.3-m canopy (leaf area index = 8.3) show a progressive increase in both carbon isotope discrimination and ϕ as light decreases. A similar increase was observed at the ecosystem scale when we used eddy covariance net ecosystem CO_2 fluxes, together with isotopic profiles, to partition photosynthetic and respiratory isotopic flux densities (isofluxes) and derive canopy carbon isotope discrimination as an integrated proxy for ϕ at the canopy level. Modeled values of canopy CO_2 fixation using leaf-level measurements of ϕ suggest that around 32% of potential photosynthetic carbon gain is lost due to light limitation, whereas using ϕ determined independently from isofluxes at the canopy level the reduction in canopy CO_2 uptake is estimated at 14%. Based on these results, we identify ϕ as an important limitation to CO_2 uptake of crops with the C_4 pathway.

Biomass production by perennial plant species can abate greenhouse gas emissions either by increased carbon sink activity and soil organic carbon sequestrations or by displacing fossil fuel emissions in the production of static energy (U.S. Department of Energy, 2006; Somerville, 2007). Perennial plant species with the C_4 photosynthetic pathway combine high productivity and resource use efficiency with low requirements for agronomic inputs; thus, they seem well equipped for biomass-based energy production (Lobell et al., 2008). For instance, *Miscanthus* (*Miscanthus* × *giganteus* hybrid) is a perennial C_4 grass with a recorded annual dry matter production up to 4 kg m^{-2} (Heaton et al., 2004a, 2004b).

Thus, attributes of the C_4 pathway (potentially high productivity coupled with high nitrogen and water use efficiencies; Sage, 2004) can be coupled to the carbon sequestration potential of a rhizomatous perennial (Hansen et al., 2004; Clifton-Brown et al., 2007). *Miscanthus* has higher productivity than switchgrass (*Panicum virgatum*; Heaton et al., 2004a) and has sufficient cold tolerance (Beale et al., 1996; Naidu et al., 2003; Wang et al., 2008a, 2008b) for cultivation in temperate climatic conditions. However, we hypothesized that growth at low temperatures and low light in a temperate climate may reduce the conversion efficiencies of such a crop, and we set out to explore the specific limitations that may occur due to shading in a crop with a high leaf area index.

Our study focused on the leakiness (ϕ) of bundle sheath (BS) cells to CO_2 as a potential bottleneck in the photosynthetic performance of a *Miscanthus* canopy. The carbon-concentrating mechanism inherent to the C_4 pathway relies on spatial separation of carboxylases between mesophyll (M) cells (phospho*enol*pyruvate carboxylase) and BS cells (Rubisco). Decarboxylation of organic acids within the BS generates high CO_2 concentrations adjacent to Rubisco, thereby suppressing oxygenase activity, but some of this CO_2 retrodiffuses and is refixed within the M cells. Such ''leakage'' in the system occurs through the BS cell walls, facilitated by the symplastic connections between M and BS, which are required for metabolite exchanges. Estimates for BS ϕ at the leaf level range between 10% and 40% (Osmond and Smith, 1976; Farquhar, 1983;

[1] This work was supported by the Alexander James Keith Studentship and the European Framework Program Infrastructure for Measurement of the European Carbon Cycle through Trinity College Dublin, Department of Botany (to J.K.).

* Corresponding author; e-mail wk229@cam.ac.uk.

The author responsible for distribution of materials integral to the findings presented in this article in accordance with the policy described in the Instructions for Authors (www.plantphysiol.org) is: Johannes Kromdijk (wk229@cam.ac.uk).

[W] The online version of this article contains Web-only data.

[OA] Open Access articles can be viewed online without a subscription.

www.plantphysiol.org/cgi/doi/10.1104/pp.108.129890

Henderson et al., 1992; Hatch et al., 1995; Fravolini et al., 2002; Cousins et al., 2006, 2008; Tazoe et al., 2006, 2008; Kubasek et al., 2007). External factors associated with increasing ϕ are low temperature (Henderson et al., 1992; Kubasek et al., 2007), water stress (Farquhar, 1983; Bowman et al., 1989; Buchmann et al., 1996), low nitrogen nutrition (Meinzer and Zhu, 1998), and, most markedly, low light (Henderson et al., 1992; Buchmann et al., 1996; Cousins et al., 2006, 2008; Tazoe et al., 2006, 2008; Kubasek et al., 2007).

The loss of C_4 efficiency under low photon flux density (PFD) was recently quantified in a series of laboratory measurements and theoretical modeling studies (Von Caemmerer, 2000; Cousins et al., 2006, 2008; Tazoe et al., 2006, 2008) using real-time carbon isotope discrimination ($\Delta^{13}C$). However, it is not clear if the increase in ϕ results initially from light limitation of Rubisco activity, relative to phospho*enol*pyruvate carboxylase activity, or increased Rubisco oxygenase and photorespiratory costs, or the ATP requirement for phospho*enol*pyruvate regeneration (Von Caemmerer and Furbank, 2003), and whether this phenomenon occurs transiently or permanently following the transfer from high-light to low-light conditions.

In this study, we set out to quantify the extent of ϕ during gas exchange at leaf and canopy scale for a 13-year-old *Miscanthus* stand at Teagasc Oak Park (Carlow, Ireland). Short-term field measurements of gas exchange and $\Delta^{13}C$ at leaf level were used to compute ϕ and the corresponding loss of carbon assimilation under field conditions using the model for C_4 photosynthesis by Von Caemmerer and Furbank (1999) and Von Caemmerer (2000). In parallel, canopy isotopic flux densities, or "isofluxes" (CO_2 flux multiplied by isotopic signature), were constructed using eddy covariance data combined with [CO_2] and $\delta^{13}C$ (carbon isotope composition relative to Vienna Pee Dee Belemnite standard) diurnal vertical profile measurements within the canopy and used to derive canopy $\Delta^{13}C$ and ϕ values. We infer that while the effect of ϕ is higher at leaf level when measured in a well-coupled cuvette, potential carbon uptake is still significantly reduced by ϕ when assessed at the canopy scale. We conclude that leakage represents a considerable constraint on C_4 productivity, particularly in temperate climates, which is especially significant when the current and future importance of the C_4 pathway for food production (e.g. maize [*Zea mays*], sorghum [*Sorghum bicolor*], sugarcane [*Saccharum officinarum*]) and bioenergy production and CO_2 mitigation (*Miscanthus*, switchgrass) is taken into account.

RESULTS

Canopy Development

In Figure 1, we show the vertical distribution of leaf area through the canopy. The total leaf area index for the canopy was 8.3 ± 0.51 $m^2\ m^{-2}$. A large proportion of this leaf area (2.8 ± 0.54 $m^2\ m^{-2}$) was located between 2 and 3 m height, with a smaller proportion (1.4 ± 0.49 $m^2\ m^{-2}$) located between 1 and 2 m. The section between 0 and 1 m also had a substantial fraction of the total leaf area (3.2 ± 0.80 $m^2\ m^{-2}$).

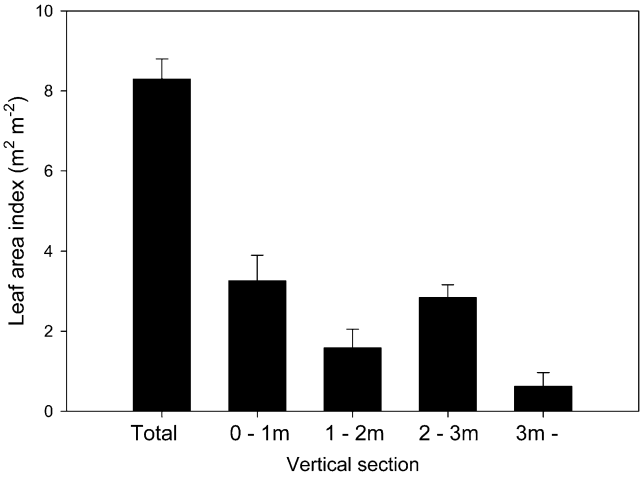

Figure 1. Total leaf area index ($m^2\ m^{-2}$) and leaf area index separated into 1-m vertical sections. Error bars indicate 1 SD.

Potential Rate of Photosynthesis

In Figure 2, photosynthetic CO_2 uptake is depicted by electron transport capacity (J; determined using chlorophyll fluorescence; Fig. 2A) and CO_2 response (determined from gas exchange; Fig. 2B) as a function of height within the canopy. Due to the CO_2-concentrating mechanism of C_4 photosynthesis, light saturation of J (maximum electron transport capacity; J_{max}) typically occurred only at very high levels of PFD. At 3 m, J_{max} reached 142.4 ± 20.5 μequiv $m^{-2}\ s^{-1}$ at PFD of 1,769 ± 42 μmol quanta $m^{-2}\ s^{-1}$, whereas at 2.5 m, J_{max} was 104.1 ± 8.7 μequiv $m^{-2}\ s^{-1}$ at PFD of 1,834 ± 41 μmol quanta $m^{-2}\ s^{-1}$. At 2 m, J_{max} and saturating PFD were lower (54.8 ± 13.1 μequiv $m^{-2}\ s^{-1}$ at 1,205 ± 21.5 μmol quanta $m^{-2}\ s^{-1}$), and they were even lower at 1.5 m (26.6 ± 9.1 μequiv $m^{-2}\ s^{-1}$ at 919 ± 41.6 μmol quanta $m^{-2}\ s^{-1}$). At 1 m, J_{max} and saturating PFD were lowest (7.5 ± 1.8 μequiv $m^{-2}\ s^{-1}$ at 553 ± 64.0 μmol quanta $m^{-2}\ s^{-1}$), and there was very little response of J to light intensity. Mitochondrial (dark) respiration was also measured following 5 min in the dark, and averages yielded 0.89 ± 0.29 μmol $m^{-2}\ s^{-1}$ for leaves at 3-m height, 0.71 ± 0.36 μmol $m^{-2}\ s^{-1}$ for leaves at 2-m height, and 0.40 ± 0.25 μmol $m^{-2}\ s^{-1}$ for leaves at 1-m height.

While J_{max} at 2.5 and 2 m was reduced to 73% and 38% of values at 3 m, maximum photosynthetic capacity (A_{max}; Fig. 2B) values at 2.5 and 2 m were 113% and 74% of those at 3 m. Similarly, carboxylation efficiency (CE), calculated from the initial slopes of the CO_2 response curves (Fig. 2B), was 0.13 μmol $CO_2\ m^{-2}\ s^{-1}$ mol μmol^{-1} at 3 m, 0.15 at 2.5 m, and 0.08 at 2 m. Below 2 m, CE decreased sharply to 0.04 at 1.5 m and 0.007 at 1 m, with a clear separation in CO_2 response between lower and

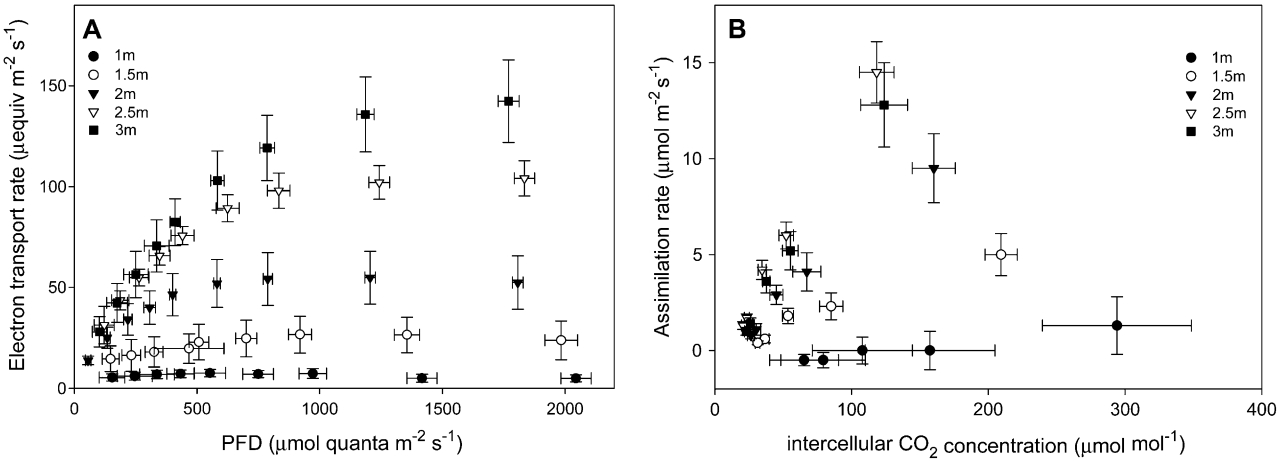

Figure 2. A, Electron transport rate (*J*) at different levels of incident PFD for leaves at 1-, 1.5-, 2-, 2.5-, and 3-m height. Error bars indicate 1 SD. B, Light-saturated photosynthetic assimilation rates at different leaf intercellular CO_2 concentrations for leaves at 1-, 1.5-, 2-, 2.5-, and 3-m height. Measurements were taken at 1,600 μmol m^{-2} s^{-1} PFD and 22°C, and vapor pressure deficit was kept below 1 kPa.

higher leaf cohorts. Thus, whereas the light response of *J* had acclimated to a markedly lower capacity above 2 m, the transition in the decline of A_{max} and carboxylation efficiency occurred lower in the canopy.

Realized Rate of Photosynthesis

Vertical profiles of net CO_2 assimilation (A_n; Fig. 3, A–E), transpiration (E; Fig. 3, F–J), and stomatal conductance (g_s; Fig. 3, K–O), measured in situ on leaves throughout the canopy, are shown as a function of incident PFD. The observations reflected a steep light gradient within the canopy, with incident PFD below 2.5 m seldom higher than 50 μmol quanta m^{-2} s^{-1}. High in the canopy at 3 m, A_n frequently was light saturated (10–12 μmol CO_2 m^{-2} s^{-1}; Fig. 3A). At 2.5 m, most CO_2 fixation (3–8 μmol CO_2 m^{-2} s^{-1}) occurred at PFD lower than 500 μmol quanta m^{-2} s^{-1} (Fig. 3B). Leaves at 2 m (Fig. 3C) were subject to very low light levels (0–75 μmol quanta m^{-2} s^{-1}), but reasonable values of A_n were still sustained (0–7 μmol CO_2 m^{-2} s^{-1}). At 1 and 1.5 m, the colimitation of light intensity and photosynthetic capacity clearly reduced A_n (0–2 μmol CO_2 m^{-2} s^{-1}; Fig. 3, D and E).

At 2.5 and 3 m, g_s ranged between 0.05 and 0.15 mol m^{-2} s^{-1} (Fig. 3, K and L), with generally higher conductances at 3 m than at 2.5 m for comparable light levels, which correspondingly led to higher rates of water loss in leaves at 3 m (Fig. 3, F and G). At 1 and 1.5 m, g_s remained below 0.03 mol m^{-2} s^{-1} (Fig. 3, N and O), and it increased to just above 0.06 mol m^{-2} s^{-1} at 2 m (Fig. 3M), but only for light levels above 50 μmol quanta m^{-2} s^{-1}. Corresponding transpiration rates were less than 0.4 mmol water m^{-2} s^{-1} for leaves at 1 and 1.5 m (Fig. 3, I and J) and increased with light intensity to 1.5 mmol water m^{-2} s^{-1} at 2 m (Fig. 3H).

In conclusion, leaves at 2.5 and 3 m receive higher incident PFD than leaves at lower locations and consequently exhibit much higher in situ rates of CO_2 fixation and water loss than leaves at 1 and 1.5 m, while leaves at 2 m frequently achieve comparable assimilation and transpiration rates to leaves higher in the canopy.

Leaf $\Delta^{13}C$ and ϕ

In Figure 4, we show the results for instantaneous $\Delta^{13}C$ and corresponding ratios of intercellular CO_2 and ambient CO_2 partial pressures (p_i/p_a) from gas exchange. Also, corresponding derived values of ϕ are shown (derived from Eq. 3 below). $\Delta^{13}C$ observations for individual leaves covered a wide range of values. $\Delta^{13}C$ above 350 μmol quanta m^{-2} s^{-1} PFD showed some variation (Fig. 4A), ranging between 2.6‰ and 6.9‰. At lower PFD, $\Delta^{13}C$ measurements were much more variable, ranging from 0.5‰ (1.5 m) to 16.5‰ (1 m). There was also a wide range of p_i/p_a values derived from gas exchange during the isotopic determinations, ranging from 0.25 (high PFD, high in the canopy) to 0.8 (shaded leaves, low in the canopy). BS ϕ to CO_2, derived from p_i/p_a and $\Delta^{13}C$ using Equation 3 below, showed a similar trend (Fig. 4C), with relatively lower values of ϕ above 350 μmol quanta m^{-2} s^{-1} PFD higher in the canopy and a wide range of values below this threshold light intensity lower in the canopy. At higher light intensity, ϕ was mostly between 0.2 and 0.5 for leaves at 3 m. Below 350 μmol quanta m^{-2} s^{-1} PFD, the range for ϕ increased with values up to 0.8 (specifically found at 1 m and 48 μmol quanta m^{-2} s^{-1}).

Canopy CO_2 Uptake, $\Delta^{13}C$, and ϕ

In Figure 5, we present eddy covariance flux measurements of ecosystem CO_2 exchange with corresponding levels of incident PFD as well as canopy $\Delta^{13}C$ (derived with the eddy covariance-flask method, as described by Bowling et al. [2003]). Except for

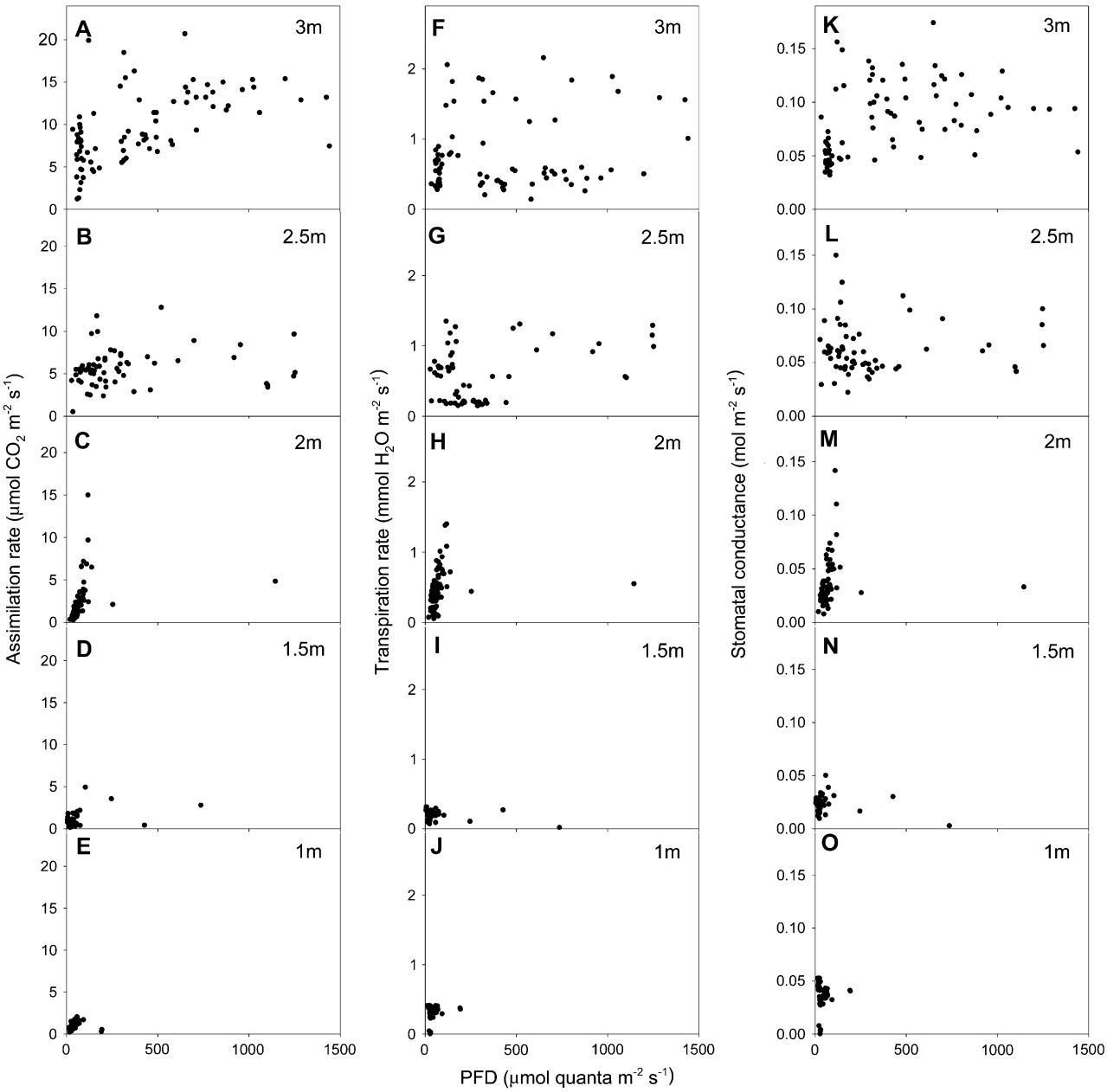

Figure 3. Steady-state levels for photosynthetic assimilation rate (A–E), transpiration rate (F–J), and stomatal conductance (K–O) at different levels of incident PFD. Measurements were taken under field conditions for leaves at (bottom to top) 1-m (n = 53), 1.5-m (n = 59), 2-m (n = 91), 2.5-m (n = 64), and 3-m (n = 84) height.

measurements in the early morning and late afternoon, the canopy was thoroughly mixed and storage flux below the eddy covariance measurements was insignificant (determined by vertical profile measurements of CO_2 concentrations within the canopy), apart from measurements between 6:00 and 7:00 AM and between 6:00 and 7:00 PM, which were not used for canopy $\Delta^{13}C$ determinations.

Ecosystem net CO_2 exchange (Fig. 5B) showed a clear diurnal pattern, with nocturnal respiration mainly correlated with temperature (1°C bin-averaged r^2 = 0.887) and net uptake mostly controlled by incident PFD (Fig. 5A). The $\delta^{13}C$ of ecosystem respiration was determined by taking the y intercept of a Keeling plot (linear geometric mean regression of $1/[CO_2]$ versus $\delta^{13}C$) assuming a two-source mixing model (Keeling, 1958, 1961). For our 13-year-old stand (Table I), $\delta^{13}C$ of respiration was still very much influenced by a C_3 carbon isotope signal from the previous cropping system, which is consistent with the low turnover of soil organic carbon in *Miscanthus* ecosystems (Hansen et al., 2004; Clifton-Brown et al., 2007).

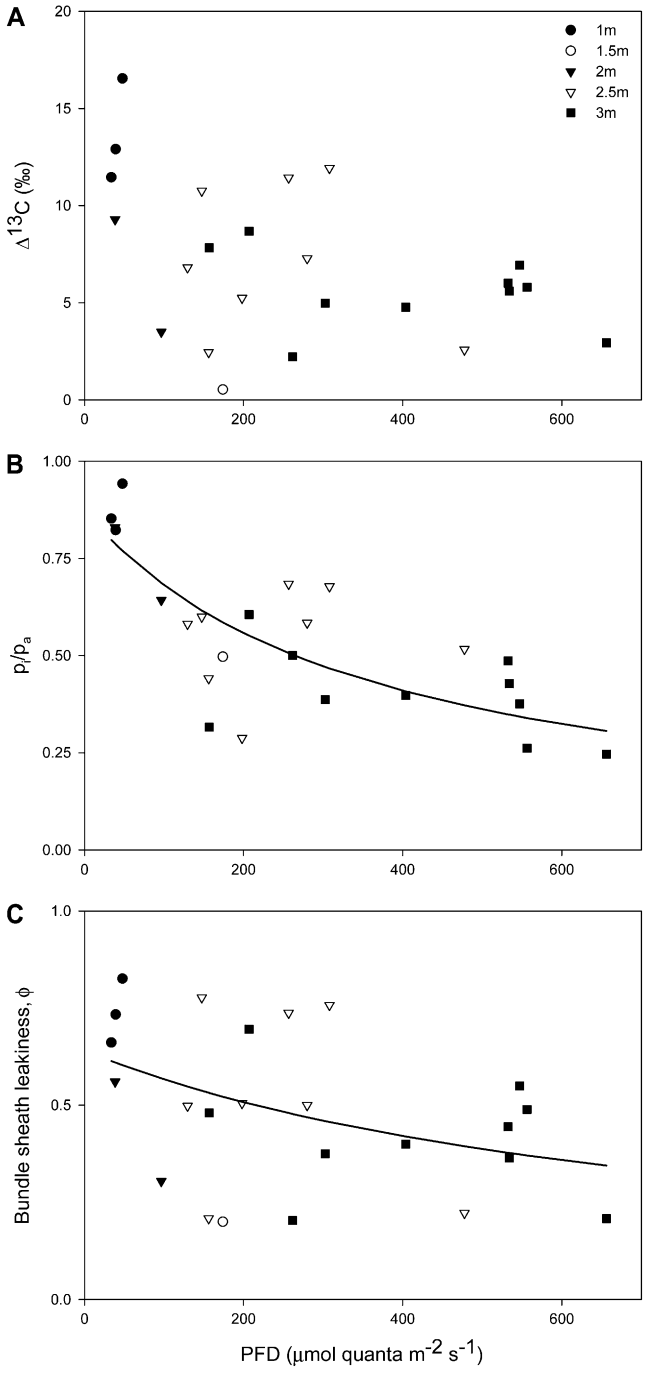

Figure 4. A, Short-term $\Delta^{13}C$ measured concurrently with gas exchange at natural light intensity for leaves at 1-m ($n = 3$), 1.5-m ($n = 1$), 2-m ($n = 2$), 2.5-m ($n = 8$), and 3-m ($n = 9$) height. B, Ratio between internal and ambient CO_2 mole fractions. The line plot represents nonlinear regression [$p_i/p_a = (a \times b)/(b + \text{PFD})$, where $a = 0.8738$, $b = 353.2301$, $r^2 = 0.55$] used in Figure 6 to calculate canopy ϕ. C, ϕ calculated with Equation 1 using measurements of $\Delta^{13}C$ (A) and the ratio between internal and ambient CO_2 mole fractions (B). The line plot shows the best fit of ϕ [$(a \times b)/(b + \text{PFD})$, where $a = 0.6409$, $b = 763.0974$, $r^2 = 0.16$] used in Figure 6 to calculate A_n.

Canopy $\Delta^{13}C$ followed a diurnal trend, with lower values around midday and slightly increased values in morning and afternoon (Fig. 5C). Figure 5D shows the canopy $\Delta^{13}C$ determinations as a function of incident PFD, revealing a similar pattern as the measurements of leaf $\Delta^{13}C$ (Fig. 4A). Except for two outliers, canopy $\Delta^{13}C$ remained between 1.3‰ and 4.3‰ above 350 μmol m^{-2} s^{-1} PFD. Below this light intensity, the range of canopy $\Delta^{13}C$ values steadily expanded, with values between 1.5‰ and 6.3‰.

Losses of Potential CO_2 Fixation Due to ϕ

Canopy A_n was modeled (according to the model by Von Caemmerer and Furbank [1999] and Von Caemmerer [2000], with some adjustments; see Supplemental Appendix S1) for 3 d to show how ϕ would reduce net carbon gain on the basis of either the leaf or canopy data presented above (Figs. 4 and 5, respectively; hereafter referred to as "leaf level" and "canopy level"). Measured vertical canopy profiles of temperature, PFD, and photosynthetic capacity were used to compute a vertical profile of A_n, which was then multiplied by leaf area at each height and summed to obtain canopy A_n. Expression of individual leaves in canopy A_n, therefore, was weighted by their assimilation rate. In order to estimate the impact of ϕ, we calculated theoretical values for canopy A_n without leakage ($\phi = 0$) and compared these values with canopy A_n obtained with our estimates for ϕ at leaf or canopy level (Fig. 6A).

In Figure 6A, the 100% datum represents canopy A_n with ϕ set to zero. Both leaf- and canopy-level modeled values of canopy A_n were reduced because of ϕ. When canopy A_n was calculated with the use of ϕ based on canopy-level determinations, the reduction due to leakage was lower than when canopy A_n was derived from leaf-level measurements. The decrease in canopy A_n would be most severe when light was limiting early in the morning or in the evening, when canopy A_n was predicted to be only 43% (leaf level) or 62% (canopy level) of canopy A_n without leakage of CO_2. Canopy A_n at midday was predicted to range from 85% (leaf level) to 94% (canopy level) of canopy A_n without leakage.

In order to assess the cumulative effect of ϕ, A_n was also summed over 3 d. Cumulative canopy A_n was 68% (leaf level) to 86% (canopy level) of canopy A_n without CO_2 leakage (Fig. 6B), indicating that cumulative losses of canopy CO_2 fixation due to ϕ over 3 d were between 14% and 32%.

DISCUSSION

This study makes a major contribution to understanding the constraints to CO_2 uptake within *Miscanthus*, an important biomass crop. We have evaluated the impact of ϕ, an intriguing physiological correlate of the C_4 pathway, which has previously been investigated largely under laboratory conditions. The data have demonstrated that ϕ provides a significant constraint

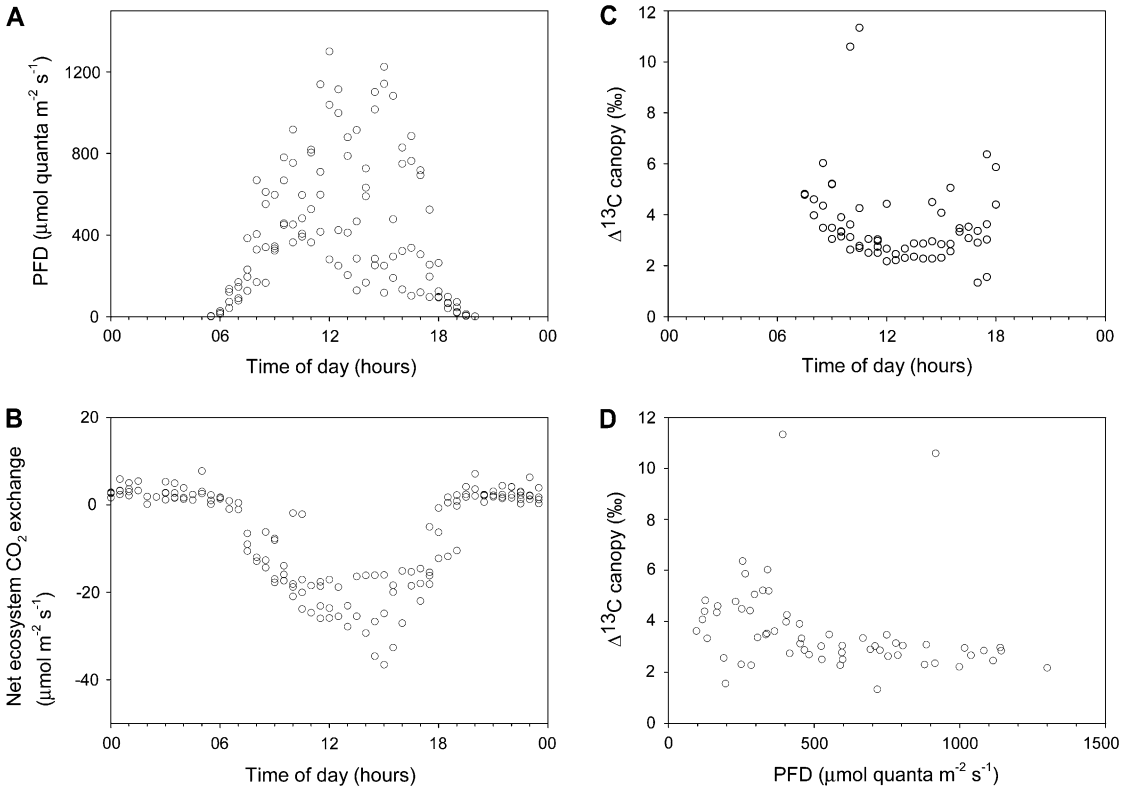

Figure 5. Accumulated data for August 28 to September 1, 2007. A, Incident PFD. B, Eddy covariance measurements of net ecosystem CO_2 exchange. Direction of net flux is indicated by plus/minus sign, and negative (positive) flux indicates net CO_2 uptake (net respiration). C, Canopy $\Delta^{13}C$ calculated by assigning isotopic signatures (from regressions in Table I) to gross CO_2 uptake derived from daytime net CO_2 fluxes (B) and ecosystem respiration based on nighttime regression with soil temperature ($y = 0.5505e^{0.0748T}$; $r^2 = 0.887$). D, Canopy $\Delta^{13}C$ (C) as a function of incident PFD.

to carbon assimilation at leaf and canopy level under field conditions when estimated using real-time $\Delta^{13}C$ techniques. We now evaluate the implications of our findings for integrating leaf-level and canopy-level gas-exchange processes and scaling likely physiological constraints to *Miscanthus* productivity in a temperate climate.

Gas Exchange and Fluorescence

Measurements of assimilation rate under controlled conditions comply well with previous findings. The high-light saturation points in Figure 2A are consistent with reported values for C_4 photosynthesis (Usuda, 1987; Beale et al., 1996, 1997). Carboxylation efficiency under saturating light (initial slope; Fig. 2B) as well as gas exchange under field conditions (Fig. 3) at 3 and 2.5 m agreed with findings by Beale et al. (1996, 1997) for the third leaf of *Miscanthus* (top down) during the second half of the growing season. Below 2 m, A_n decreased rapidly, which can be explained by leaf age and associated lower enzymatic activity (Usuda, 1984) as well as by early stages of leaf senescence at 1-m height. At canopy level, half-hourly averages of net ecosystem exchange were consistent with long-term measurements above *Miscanthus* (F. Carroll and M.B. Jones, unpublished data).

In the absence of simultaneous measurements of A_n and J under field conditions, we are not able to make any direct comparison of how A_n responded to changes in light use efficiency caused by ϕ. Also, measurements of the quantum yield of PSII are known to be influenced by quantitative and qualitative light history of the leaf as well as leaf temperature (Edwards and Baker, 1993). Figure 2B was determined under steady-state laboratory conditions, and so interpolating the ratio of J versus A_n, which should increase at low PFD based on our ϕ determinations (assuming that cyclic

Table I. *Regressions to derive ecosystem gross fluxes (values of parameters ± SE)*

Regression	Intercept	Slope	r^2	No.
Nocturnal Keeling plot	−25.885 ± 0.801	6,334 ± 318	0.942	25
Daytime [CO_2] versus $\delta^{13}C$	13.519 ± 2.441	−0.06031 ± 0.00673	0.776	20

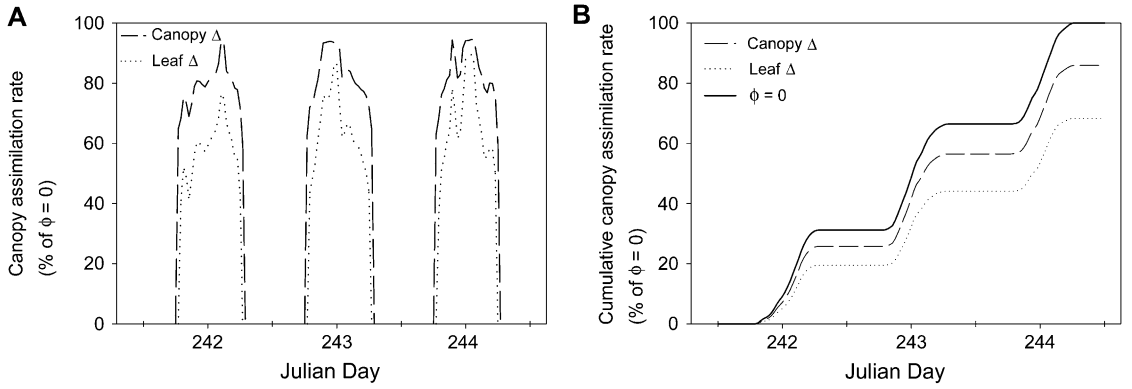

Figure 6. Results for August 29 to August 31, 2007 (Julian days 242–244). A, Modeled canopy A_n for two scenarios: ϕ based on leaf level measurements of $\Delta^{13}C$ and on canopy $\Delta^{13}C$ (rates are depicted as percentages of $\phi = 0$). ϕ is taken from regression $\phi = a \times b/(b + \text{PFD})$, where $a = 0.6409$ and $b = 763.0974$ for leaf level (Figure 4C) and $a = 0.4014$ and $b = 470.342$ for canopy level (based on nonlinear fit of the canopy model in Figure 5C, using Eq. 3). B, Cumulative modeled canopy A_n for $\phi = 0$, based on leaf level measurements of $\Delta^{13}C$ and on canopy $\Delta^{13}C$. Scenarios are compared with total cumulative canopy A_n with $\phi = 0$.

electron flow occurs at a constant fraction of J and absence of other significant electron sinks), could only be inferred on a qualitative basis. However, we note that for a fast-growing crop, leaves that were previously fully exposed were subsequently shaded by the developing canopy. For our observations of *Miscanthus*, it was evident that J_{max} was down-regulated higher in the canopy (2.5 m), while photosynthetic capacity (CE, A_{max}) was sustained lower in the canopy (2 m). The implications for the effect of ϕ on the ratio between J and A_n, therefore, need to be addressed in a more detailed study.

$\Delta^{13}C$

At high PFD (above 350 μmol quanta m^{-2} s^{-1}), $\Delta^{13}C$ for leaves at different heights matched well with values generally assigned to C_4 photosynthesis (for reviews, see Farquhar, 1983; O'Leary, 1988). $\Delta^{13}C$ at lower PFD tended to be much more variable, ranging from 0.5‰ (1.5 m) to 16.5‰ (1 m), which is consistent with likely changes in the coupling of C_4 and C_3 cycles, variations in photosynthetic capacity, local microenvironment, and associated enzyme activity between leaves. Also, $\Delta^{13}C$ for individual leaves, when calculated using Equation 4 below, becomes increasingly less precise when CO_2 depletion is low relative to the CO_2 concentration in air. The observation that higher values of $\Delta^{13}C$ seemed to occur more often at low PFD deep in the canopy is consistent with previously reported values under low PFD for *Amaranthus cruentus* (Tazoe et al., 2006, 2008) and *Flaveria bidentis* (Cousins et al., 2006).

Remarkably, the increase in $\Delta^{13}C$ at low PFD was also observed when derived independently at canopy level. Canopy $\Delta^{13}C$ mostly reflected $\Delta^{13}C$ processes by leaves high in the canopy. Since $\Delta^{13}C$ at leaf level is weighted in canopy $\Delta^{13}C$ according to the rate of CO_2 uptake relative to other leaves, predictably leaves high in the canopy with higher assimilation rates influence canopy A_n and $\Delta^{13}C$ more than leaves at lower locations. The method used to determine canopy $\Delta^{13}C$ (Bowling et al., 2003) depended on measurements of ecosystem CO_2 exchange together with isotopic compositions of ecosystem respiration and daytime canopy air. A single isotopic respiratory signal had to be assumed for the complete ecosystem, which is likely to be an oversimplification, given the difference between current (C_4) and previous (C_3) vegetation on soil respiration (Buchmann and Ehleringer, 1998) and light effects on respiration of aboveground biomass (Atkin et al., 1998).

The ecosystem respiratory flux was defined by an exponential regression between soil temperature and nocturnal eddy covariance measurements of CO_2 efflux (Lloyd and Taylor, 1994), which could only be firmly established by bin averaging the ecosystem respiration measurements in 1°C increments. A similar problem was found by Bowling et al. (2003) and appears to be quite common in previous reports of net ecosystem partitioning into gross assimilation and respiration fluxes (Reichstein et al., 2005; Knohl et al., 2008). Bowling et al. (2003) explained part of the variability by spatial variation of soil moisture content, and Knohl et al. (2008) implied nonhomogeneity of the soil profile. Both factors may have contributed in our study, especially since diurnal measurements of soil respiration as well as soil temperature and moisture content were also spatially variable (data not shown).

Increased $\Delta^{13}C$ at Low Light Intensity

Our results support previous observations of an increase in $\Delta^{13}C$ at low light intensity. The underlying mechanisms have been analyzed extensively. Based on studies of photosynthetic behavior in C_4 plants, Leegood et al. (1989) argued that the energy supply for the assimilatory pathway (production of ATP and NADPH) declines drastically following a transition from high to low PFD. Stimulation of cyclic electron flow and Q-cycle activity (Furbank et al., 1990) might make up for part of the ATP shortage (by cyclic par-

titioning of electrons around the PSI complex and altering the ATP-NADPH production ratio). However, we can find no evidence in the literature for increased activity of these alternative electron cycling processes as a result of lower PFD; so ultimately, photosynthesis remains limited by the energy supply.

Energy limitation could increase measured $\Delta^{13}C$ in several ways. First, an increase in the relative contribution from mitochondrial respiration under low light could vary $\Delta^{13}C$ (Duranceau et al., 2001), particularly if respiratory CO_2 is enriched in ^{13}C (Ghashghaie et al., 2003). Alternatively, Henderson et al. (1992) stated that with reduced phospho*enol*pyruvate regeneration slowing C_4 cycle activity under low light, a decrease in the BS CO_2 concentration or CO_2-O_2 ratio would allow the relative contribution of photorespiration to increase. The extra energy needed for the photorespiratory cycle would limit C_3 cycle activity compared with C_4 cycle activity, which would lead to an increase in leakage of CO_2 (Von Caemmerer et al., 1997a, 1997b) from BS cells, thereby allowing more of the isotopic fractionation by Rubisco (30‰) to be expressed. Recently, Tazoe et al. (2008) may have provided evidence for an increase in ϕ as a result of energy limitation under low PFD, since the increase in $\Delta^{13}C$ and, hence, ϕ, following a transfer to low PFD, was lower in *Amaranthus cruentus* plants grown under low light intensity compared with high-light-grown plants. This may have been caused by a slightly altered relative composition (within the limits of C_4 pathway plasticity) of the photosynthetic apparatus in the plants grown under low PFD, resulting in an improved ability to sustain carboxylation efficiency in BS cells at low light. The relative changes in light use and carboxylation efficiency within the canopy (Fig. 2; see discussion above) certainly suggest that differing degrees of acclimation occur at reduced light intensity, once fully expanded leaves are overtopped by the newly growing canopy.

BS ϕ

At high light intensity, ϕ was similar to reported values in NADP-malic enzyme C_4 photosynthesis of 0.2 to 0.3 in maize (Henderson et al., 1992) and 0.3 to 0.4 in sugarcane (Meinzer et al., 1994; Meinzer and Saliendra, 1997). The maximum values for ϕ at low light intensity (below a threshold PFD of 350 μmol quanta $m^{-2} s^{-1}$) were comparable to reported values of 0.65 at 150 μmol quanta $m^{-2} s^{-1}$ for *F. bidentis* by Cousins et al. (2006) and of 0.76 at 40 μmol quanta $m^{-2} s^{-1}$ for *A. cruentus* by Tazoe et al. (2008). Other contributions to the measured leaf-level variability of $\Delta^{13}C$ and ϕ could be related to the input parameters (p_i/p_a, b_4, b_3, s, and a) and simplifying assumptions for Equation 3 below. The assigned parameter value of −6‰ (at 22°C) to b_4 is based on the assumption that carbonic anhydrase (CA) is abundant enough to maintain isotopic equilibrium between CO_2 and HCO_3^-. However, if CA activity is too low to maintain equilibrium, b_4 becomes less negative and $\Delta^{13}C$ increases (leading to an overestimation of ϕ with Eq. 3), which was shown by Cousins et al. (2006) with *F. bidentis* RNA antisense CA plants. Von Caemmerer et al. (2004) argued that CA activity was too high to maintain steady-state assimilation rates in *F. bidentis*; however, Gillon and Yakir (2000, 2001) have reported that CA activity in C_4 monocots could limit photosynthetic rates. Equation 3 requires high CO_2 concentration in BS cells relative to that in M cells. If this requirement was not met, ϕ might have been overestimated by 10% or more for very low BS CO_2 concentrations (Tazoe et al., 2008). Also, the gradient between intercellular and M CO_2 concentrations was assumed to be negligible in Equation 3. Results of a sensitivity analysis with the extended model by Farquhar (1983) showed that a gradient of 30 μmol mol^{-1} would cause a mean absolute difference in calculated ϕ of 0.026.

Furthermore, there might be additional fractionations associated with photorespiration (Gillon and Griffiths, 1997; Lanigan et al., 2008), variable mitochondrial respiration between old and young leaves (Villar et al., 1995), or different carbon sources for respiration (Ghashghaie et al., 2003). A sensitivity analysis (Table II) was undertaken, using the extended model by Farquhar (1983), with various combinations of values for mitochondrial respiration, the fractionation factor assigned to respiration (e), and carboxylation rate in BS cells (V_c). The results were relatively insensitive to most of the modeled combinations, and only when V_c was low (3 μmol $m^{-2} s^{-1}$) and mitochondrial respiration was high (1.2 μmol $m^{-2} s^{-1}$) did mean absolute differences in ϕ range from −0.06 to 0.08 (depending on the value of e; Table II). The observed dark respiration rate in leaves at 1, 2, and 3 m in our study (0.40, 0.71, and 0.89 μmol $m^{-2} s^{-1}$, respectively) suggest that such errors would not occur, due to the relative reduction in both assimilation and respiration rates low in the canopy.

Table II. *Sensitivity of leaf level calculations of ϕ to different values of mitochondrial respiration rate (R_d), fractionation factor associated with mitochondrial respiration (e), and carboxylation rate in BS cells (V_c)*

The extended model by Farquhar (1983) was used to calculate the mean absolute difference of ϕ between the extended model and the simplified version without respiratory fractionation (Eq. 3). Phospho*enol*pyruvate carboxylation and photorespiration rates were set at 1.5 and 0.03 times V_c, respectively. A value of 11.5‰ was used for the fractionation factor associated with photorespiration, based on recent estimates by Lanigan et al. (2008).

R_d	e	V_c	Mean Difference in ϕ
$\mu mol\ m^{-2}\ s^{-1}$	‰	$\mu mol\ m^{-2}\ s^{-1}$	
0.4	6	30	0.0080
0.4	−6	30	0.0032
0.4	6	3	0.0306
0.4	−6	3	−0.018
1.2	6	30	0.0129
1.2	−6	30	−0.0016
1.2	6	3	0.0852
1.2	−6	3	−0.0614

Implications of Results for Canopy CO_2 Fixation

Assuming that ϕ is the major correlate of variations in leaf and canopy $\Delta^{13}C$, we suggest that ϕ significantly reduces canopy net assimilation rate. Having calculated ϕ from leaf-level $\Delta^{13}C$ and simultaneous gas exchange, and also independently from canopy $\Delta^{13}C$ and PFD and temperature measurements within the canopy, there were relative reductions in cumulative canopy A_n ranging from 14% to 32%. There are implications for losses of carbon-fixing capacity in densely planted C_4 crops. Screening for varieties with low $\Delta^{13}C$ under a range of limiting light conditions might be a means to increase the productivity of *Miscanthus* (or other C_4 crops), especially in the temperate climate conditions of northwestern Europe. Additionally, the observed variations in the canopy profile of J_{max} and A_{max} may provide a mechanistic understanding of the energetic factors controlling ϕ.

In conclusion, our results have established that retrodiffusion or leakage of CO_2 from BS cells is a major limitation to carbon gain at leaf and canopy scales under field conditions. While additional laboratory studies are required to evaluate the exact nature of this energetic inefficiency at low light (perhaps through the analysis of transient responses of ϕ to light in sun- and shade-acclimated plants), there was an agreeable consistency in response to incident PFD measured independently for individual leaves and their cumulative light limitation within the upper part of a full C_4 crop canopy. Second, we have been able to demonstrate how ϕ, as a function of leaf area index and incident PFD within the canopy, can be translated into canopy-scale carbon partitioning and potential productivity. Additional work is required to confirm the consistency of these responses during canopy development and to allow more precise partitioning between respiratory components and canopy net assimilation. However, carbon isotopes have provided a powerful means to analyze instantaneous photosynthetic limitation at leaf and canopy scale and allowed us to derive estimates of the likely reduction due to ϕ in CO_2 uptake for a C_4 crop limited by light and temperature in a northern temperate environment. The good agreement between previous measurements of ϕ versus PFD from controlled environment studies (Henderson et al., 1992; Meinzer et al., 1994; Meinzer and Saliendra, 1997; Cousins et al., 2006; Tazoe et al., 2008) and our observations under field conditions might also suggest that within-canopy measurements of PFD can be used as a rough proxy for ϕ losses due to light limitation arising from self shading.

MATERIALS AND METHODS

Site Description

Measurements were carried out at Teagasc Agricultural Research Centre (Oak Park, Carlow, Ireland) on a 13-year-old stand of *Miscanthus* (*Miscanthus* × *giganteus*) in the summer of 2007. The plot was rainfed and unfertilized except for one application of 50 kg ha^{-1} nitrogen fertilizer in 2006. Harvest of previous-year stems took place in early April 2007.

Potential Rate of Photosynthesis

Five leaves were randomly selected from 1-, 1.5-, 2-, 2.5-, and 3-m height within the canopy to assess electron transport rate (J; μmol m^{-2} s^{-1}) as a function of incident PFD. All measurements were done just above the end of the visible mid rib. First, the quantum yield of PSII (Φ_{PSII}) was measured using pulse amplitude-modulated (PAM) chlorophyll fluorescence at a range of light intensities with a mini-PAM photosynthetic yield analyzer (Heinz Walz) according to Genty et al. (1989):

$$\Phi_{PSII} = (F_m' - F_t)/F_m' \quad (1)$$

where F_m' and F_t refer to maximum fluorescence at saturating light pulse and steady-state fluorescence immediately prior to the pulse. J could then be calculated at each light level with the use of Equation 2:

$$J = \Phi_{PSII} \times PFDa \times 0.5 \quad (2)$$

where PFD represents the absorbed PFD, and 0.5 is a factor that accounts for the partitioning of energy between PSI and PSII. Leaf absorptance was set at 0.84, which has been shown to be valid for a wide range of growth conditions in *Miscanthus* (Farage et al., 2006). As a control, we also measured the chlorophyll content of different leaves ($n = 5$) from each height using the protocol by Lichtenthaler (1987), but no significant differences were found.

CO_2 responses of net assimilation rate were analyzed on three leaves that were cut at the ligule, with the cut end placed in water and recut under water, 3 cm from the base (Beale et al., 1996). The leaves were positioned in the leaf cuvette (area = 6 cm^2) of a LI6400 portable, open gas-exchange system (Li-Cor Biosciences) illuminated by a Walz Fiber Illuminator FL440 with controllable intensity, with a model 400-F fiberglass connection and projector to filter heat, and left for 30 min to acclimatize to saturating light (1,600 μmol quanta m^{-2} s^{-1}) at ambient CO_2. Leaf temperature was set at 22°C, while the vapor pressure deficit was kept below 1 kPa. After reaching steady state, the photosynthetic assimilation rate as a function of internal CO_2 concentration was determined from high to low external CO_2 concentrations (380, 150, 100, 50, and 40 μmol mol^{-1}).

Mitochondrial respiration not associated with photorespiration (R_d) was measured on different leaves from 1, 2, and 3 m ($n = 5$) by gas exchange with the LI6400 (leaf temperature set at 22°C), with readings taken after 5 min in the darkened cuvette.

Realized Rate of Photosynthesis

Leaves were randomly selected at 1-, 1.5-, 2-, 2.5-, and 3-m height within the canopy, and (still attached) photosynthetic assimilation rate, transpiration rate, and stomatal conductance were measured under natural light and temperature by placing them in the leaf cuvette of the LI6400 portable, open gas-exchange system, while being careful not to change the angle and orientation of the leaf. A reading was taken after steady state was reached (approximately 5 min).

Use of $\Delta^{13}C$ to Calculate BS ϕ

Hattersley (1976) first suggested that variation in $\delta^{13}C$ of C_4 species may reflect variations in the amount of leakage. An increase in BS ϕ results in higher $\Delta^{13}C$, because fractionation by Rubisco becomes more expressed. This relationship is used in Equation 3, developed by Farquhar (1983) and Henderson et al. (1992), which allows calculation of BS ϕ if $\Delta^{13}C$ and p_i/p_a are known.

$$\Delta = a + (b_4 + \phi(b_3 - s) - a)\, p_i/p_a \quad (3)$$

where a is the fractionation during diffusion of CO_2 in air (4.4‰), b_4 is the combined fractionation of phospho*enol*pyruvate carboxylation (2.2‰) and the isotopic equilibrium during dissolution of CO_2 and conversion to bicarbonate, yielding a net value of −6‰ (at 22°C; Mook et al., 1974), b_3 is the fractionation by Rubisco (30‰), and s (1.8‰) is the fractionation during leakage.

$\Delta^{13}C$ Measured Concurrently with Gas Exchange

To measure $\Delta^{13}C$ during gas exchange, the exhaust tube of a LI6400 portable photosynthesis system was connected to a cryogenic water and CO_2 trapping-purification line as described by Griffiths et al. (1990). CO_2 was trapped and purified for 15 min. The obtained CO_2 samples were stored in sealed glass vials and analyzed afterward with a VG SIRA dual-inlet isotope

ratio mass spectrometer (modified and maintained by Pro-Vac Services), and values were corrected for the presence of N_2O and ^{17}O. The $\delta^{13}C$ of CO_2 measured before and after photosynthetic depletion yields the net discrimination using the following equation by Evans et al. (1986):

$$\Delta^{13}C = \frac{\xi(\delta_o - \delta_e)}{1 + \delta_o - \xi(\delta_o - \delta_e)} \quad (4)$$

where

$$\xi = \frac{c_e}{c_e - c_o} \quad (5)$$

where δ_e and δ_o represent the isotopic compositions of CO_2 relative to the PDB standard, and c_e and c_o represent the CO_2 mole fractions in air entering and leaving the cuvette, respectively. The $\Delta^{13}C$ values obtained in this way thus reflect average values for 15 min of continuous photosynthetic discrimination.

Canopy Microclimate Record

A 3.5-m-tall pole with cross bars at 1-, 2-, and 3-m height was erected within the canopy with the cross bars facing north/south. PFD quantum sensors (SKP-215; Skye Instruments) were mounted on the cross bars facing south and thermocouples (Cu-Co) were mounted facing north. Also, a thermocouple and a soil moisture probe (SM200; Delta-T Devices) were inserted 0.02 m below the soil surface. A data-logger (CR21X; Campbell Scientific) was used to record and store average values every 10 min.

Another pole with air inlets on the cross bars was connected to the air inlet of a LI6400 portable, open gas-exchange system via 4-mm-diameter Teflon tubing and a switching manifold to measure and record within-canopy CO_2 concentrations at 1-, 2-, 3-, and 3.5-m height. During the recordings, the exhaust tube of the LI6400 leaf cuvette was connected to the trapping-purification line, and CO_2 was trapped and purified for 5 min and stored in sealed glass vials. The isotopic ratio of purified CO_2 was determined with a VG SIRA dual-inlet isotope ratio mass spectrometer and corrected for the presence of ^{17}O and N_2O.

Canopy Characterization

Leaf area index was measured with a Sunscan System SS-1 (Delta-T Devices). Measurements were made with the sunprobe at 0-, 1-, 2-, and 3-m height to analyze the specific leaf area index of vertical sections within the canopy as well as the total leaf area of the stand (0-m measurements).

Ecosystem CO_2 Exchange

Net ecosystem exchange (NEE) of CO_2 was measured using an eddy covariance system consisting of an open-path infrared gas analyzer (Li-Cor LI-7500) coupled to a three-dimensional sonic anemometer (Soluent R3; Gill Instruments). The sonic anemometer and air intake were positioned 1 m above the canopy. CO_2 concentrations were measured with the open-path LI-7500 infrared gas analyzer. Measurements were recorded at 20 Hz on a CR23X datalogger (Campbell Scientific), and 30-min average fluxes were processed using the EdiRe software version 1.4.3.987 (Edinburgh University). Data quality and stability were tested using the methods of Foken and Wichura (1995), and data were discarded based on a lower u* threshold of 0.1 (m s^{-1}), high SD in measured CO_2 concentration, and CO_2 concentration and flux values outside of approved bandwidths. The footprint model of Kormann and Meixner (2001) was used to determine the percentage of measured flux originating from within the measurement plot, when less than 70% of the data were discarded.

Canopy CO_2 Uptake and Isotope Discrimination

Data from diurnal measurements (August 28–29 and August 31–September 1, 2007) as well as eddy covariance flux measurements (August 28–September 1, 2007) were used to reconstruct canopy CO_2 uptake and short-term $\Delta^{13}C$ using the method described in detail by Bowling et al. (2003).

A regression (exponential, ordinary least squares) was made of nocturnal eddy covariance measurements of ecosystem respiratory fluxes against soil temperature (bin averaged per 1°C). This regression was extrapolated over daytime to partition daytime gross ecosystem respiratory flux. The daytime gross ecosystem respiratory flux was then subtracted from the daytime total net flux, measured with eddy covariance, which yielded the canopy CO_2 uptake gross flux.

We assumed that daytime net ecosystem CO_2 fluxes were composed of gross fluxes of ecosystem respiration (F_R) and canopy uptake (F_A; Eq. 6), and net ecosystem uptake fluxes were assigned a negative sign by micrometeorological convention.

$$NEE = F_R + F_A \quad (6)$$

Analogously, net isofluxes were also assumed to consist of gross respiration and photosynthetic isofluxes (Eq. 7).

$$\delta^{13}CNEE = (\delta^{13}C_R)F_R + (\delta^{13}C_a - \text{canopy}\,\Delta^{13}C)F_A \quad (7)$$

The isoflux of ecosystem respiration $[(\delta^{13}C_R)F_R]$ was determined by multiplying the daytime gross respiratory flux with the intercept of the nocturnal Keeling plot (geometric mean regression of $1/[CO_2]$ versus $\delta^{13}C$; Keeling, 1958, 1961). Net daytime isofluxes ($\delta^{13}CNEE$) were calculated by multiplying the daytime net ecosystem exchange fluxes with corresponding isotopic signatures using daytime geometric mean regression of CO_2 concentrations versus $\delta^{13}C$. Since $(\delta^{13}C_R)F_R$, $\delta^{13}CNEE$, ambient isotopic signature of CO_2 ($\delta^{13}C_a$), and gross fluxes of canopy CO_2 uptake (F_A) were identified, based on mass balance and negligible storage flux in NEE measurements (checked with diurnal vertical CO_2 concentration profiles), the isotopic contribution of canopy CO_2 uptake (δ_A) became the only unknown variable and could be solved.

Losses of Potential CO_2 Fixation Due to ϕ

We used the following approach to calculate the implications of ϕ at leaf level on canopy CO_2 uptake (A_n). Based on the leaf-level determinations, a function for hyperbolic decay $[\phi = (a \times b)/(b + PFD)]$ was fitted to define ϕ as a function of incident PFD (Fig. 4C). Measured incident PFD and temperature at 1, 2, and 3 m from August 29 to August 31 were used to represent the range of conditions defining CO_2 fixation. A vertical profile of A_n was calculated using the model for C_4 photosynthesis by Von Caemmerer and Furbank (1999) and Von Caemmerer (2000) with some adaptations (see Supplemental Appendix S1), which was multiplied by a profile of leaf area index and summed to yield canopy A_n. We calculated potential canopy A_n without CO_2 leakage ($\phi = 0$) and compared it with canopy A_n computed with ϕ determined by the fitted relationship between ϕ and PFD in Figure 4C.

A similar approach was used in combination with Equation 3 to translate measurements of canopy $\Delta^{13}C$ into ϕ for each height. First, leaf-level data were used to derive a regression between incident PFD and p_i/p_a (Fig. 4B). Based on previous results (Cousins et al., 2006; Tazoe et al., 2006, 2008) and the model by Von Caemmerer and Furbank (1999) and Von Caemmerer (2000), we used a descriptive function for hyperbolic decay $[\phi = (a \times b)/(b + PFD)]$ to describe ϕ as a function of incident PFD. The measured incident PFD within the canopy, together with Equation 3, then allowed the calculation of A_n and $\Delta^{13}C$ for each layer. $\Delta^{13}C$ weighted by A_n was used to calculate canopy $\Delta^{13}C$, which was compared with measured canopy $\Delta^{13}C$. This comparison allowed fitting parameters a and b by means of nonlinear regression, and the best fit was used to produce results for canopy A_n based on canopy-level determinations of ϕ (as described in the previous paragraph).

The Ventana Simulation Environment Vensim DSS for Windows, version 5.6a Double Precision (Ventana Systems), was used for all calculations and nonlinear regression.

Supplemental Data

The following materials are available in the online version of this article.

Supplemental Appendix S1. Modeling A_n for C_4 photosynthesis.

ACKNOWLEDGMENTS

We thank Dr. Julian Hibberd and Moritz Meyer for discussions and comments on early versions of the manuscript.

Received September 14, 2008; accepted October 23, 2008; published October 29, 2008.

LITERATURE CITED

Atkin OK, Evans JR, Siebke K (1998) Relationship between the inhibition of leaf respiration by light and enhancement of leaf dark respiration following light treatment. Aust J Plant Physiol **25:** 437–443

Beale CV, Baker MG, Farage PK, Humphries SW, Long SP (1997) Final Progress Report and Final Report of the European Miscanthus Network. University of Essex, Essex, UK, pp 1–55

Beale CV, Bint DA, Long SP (1996) Leaf photosynthesis in the C4-grass Miscanthus × giganteus, growing in the cool temperate climate of southern England. J Exp Bot **47:** 257–273

Bowling DR, Pataki DE, Ehleringer JR (2003) Critical evaluation of micrometeorological methods for measuring ecosystem-atmosphere isotopic exchange of CO_2. Agric For Meteorol **116:** 159–179

Bowman WD, Hubick KT, Von Caemmerer S, Farquhar GD (1989) Short term changes in leaf carbon isotope discrimination in salt- and water-stressed C4 grasses. Plant Physiol **90:** 162–166

Buchmann N, Brooks JR, Rapp KD, Ehleringer JR (1996) Carbon isotope composition of C4 grasses is influenced by light and water supply. Plant Cell Environ **19:** 392–402

Buchmann N, Ehleringer JR (1998) CO_2 concentration profiles, and carbon and oxygen isotopes in C_3 and C_4 crop canopies. Agric For Meteorol **89:** 45–58

Clifton-Brown JC, Breuer J, Jones MB (2007) Carbon mitigation by the energy crop, *Miscanthus.* Glob Change Biol **13:** 2296–2307

Cousins AB, Badger MR, Von Caemmerer S (2006) Carbonic anhydrase and its influence on carbon isotope discrimination during C4 photosynthesis: insights from antisense RNA in *Flaveria bidentis.* Plant Physiol **141:** 232–242

Cousins AB, Badger MR, Von Caemmerer S (2008) C_4 photosynthetic isotope exchange in NAD-ME- and NADP-ME-type grasses. J Exp Bot **59:** 1695–1703

Duranceau M, Ghashghaie J, Brugnoli E (2001) Carbon isotope discrimination during photosynthesis and dark respiration in intact leaves of *Nicotiana sylvestris*: comparisons between wild type and mitochondrial mutant plants. Aust J Plant Physiol **28:** 65–71

Edwards GE, Baker NR (1993) Can CO_2 assimilation in maize leaves be predicted accurately from chlorophyll fluorescence analysis? Photosynth Res **37:** 89–102

Evans JR, Sharkey TD, Berry JA, Farquhar GD (1986) Carbon isotope discrimination measured concurrently with gas exchange to investigate CO_2 diffusion in leaves of higher plants. Aust J Plant Physiol **13:** 281–292

Farage PK, Blowers D, Long SP, Baker NR (2006) Low growth temperatures modify the efficiency of light use by photosystem II for CO_2 assimilation in leaves of two chilling-tolerant C_4 species, *Cyperus longus* L. and *Miscanthus* x *giganteus.* Plant Cell Environ **29:** 720–728

Farquhar GD (1983) On the nature of carbon isotope discrimination in C4 species. Aust J Plant Physiol **10:** 205–226

Fravolini A, Williams DG, Thompson TL (2002) Carbon isotope discrimination and bundle sheath leakiness in three C_4 subtypes grown under variable nitrogen, water and atmospheric CO_2 supply. J Exp Bot **53:** 2261–2269

Foken T, Wichura B (1995) Tools for quality assessment of surface-based flux measurements. Agric For Meteorol **78:** 83–105

Furbank RT, Jenkins CLD, Hatch MD (1990) C4 photosynthesis: quantum requirement, C4 acid overcycling and Q-cycle involvement. Aust J Plant Physiol **17:** 1–7

Genty B, Briantais JM, Baker NR (1989) The relationship between quantum yield of photosynthetic electron transport and quenching of chlorophyll fluorescence. Biochim Biophys Acta **990:** 87–92

Ghashghaie J, Badeck FW, Lanigan G, Nogues S, Tcherkez G, Deleens E, Cornic G, Griffiths H (2003) Carbon isotope fractionation during dark respiration and photorespiration in C3 plants. Phytochem Rev **2:** 145–161

Gillon J, Yakir D (2001) Influence of carbonic anhydrase activity in terrestrial vegetation on the O-18 content of atmospheric CO_2. Science **291:** 2584–2587

Gillon JS, Griffiths H (1997) The influence of (photo)respiration on carbon isotope discrimination in plants. Plant Cell Environ **20:** 1217–1230

Gillon JS, Yakir D (2000) Naturally low carbonic anhydrase activity in C4 and C3 plants limits discrimination against $C^{18}O$ during photosynthesis. Plant Cell Environ **23:** 903–915

Griffiths H, Broadmeadow MSJ, Borland AM, Hetherington CS (1990) Short-term changes in carbon-isotope discrimination identify transitions between C3 and C4 carboxylation during Crassulacean acid metabolism. Planta **181:** 604–610

Hansen EM, Christensen BT, Jensen LS, Kristensen K (2004) Carbon sequestration in soil beneath long-term *Miscanthus* plantations as determined by ^{13}C abundance. Biomass and Bioenergy **26:** 97–105

Hatch MD, Agostino A, Jenkins CLD (1995) Measurements of leakage of CO_2 from bundle sheath cells of leaves during C4 photosynthesis. Plant Physiol **108:** 173–181

Hattersley PW (1976) Speciation and functional significance of the leaf anatomy of C4 plants. PhD thesis. Australian National University, Canberra, Australia

Heaton EA, Long SP, Voigt TB, Jones MB, Clifton-Brown J (2004a) Miscanthus for renewable energy generation: European Union experience and projections for Illinois. Mitig Adapt Strategies Glob Change **9:** 433–451

Heaton EA, Voigt T, Long SP (2004b) A quantitative review comparing the yields of two candidate C4 perennial biomass crops in relation to nitrogen, temperature and water. Biomass and Bioenergy **27:** 21–30

Henderson SA, Von Caemmerer S, Farquhar GD (1992) Short-term measurements of carbon isotope discrimination in several C_4 species. Aust J Plant Physiol **19:** 263–285

Keeling CD (1958) The concentration and isotopic abundances of atmospheric carbon dioxide in rural areas. Geochim Cosmochim Acta **13:** 322–334

Keeling CD (1961) The concentration and isotopic abundance of carbon dioxide in rural and marine air. Geochim Cosmochim Acta **24:** 277–298

Knohl A, Søe ARB, Kutsch WL, Göckede M, Buchmann N (2008) Representative estimates of soil and ecosystem respiration in an old beech forest. Plant Soil **302:** 189–202

Kormann R, Meixner FX (2001) An analytical footprint model for non-neutral stratification. Boundary-Layer Meteorol **99:** 207–224

Kubasek J, Setlik J, Dwyer S, Santrucek J (2007) Light and growth temperature alter carbon isotope discrimination and estimated bundle sheath leakiness in C4 grasses and dicots. Photosynth Res **91:** 47–58

Lanigan GJ, Betson N, Griffiths H, Seibt U (2008) Carbon isotope fractionation during photorespiration and carboxylation in *Senecio.* Plant Physiol **148:** 2013–2020

Leegood RC, Adcock MD, Doncaster HD, Hill R (1989) Analysis of the control of photosynthesis in C4 plants by changes in light and carbon dioxide. Philos Trans R Soc Lond B Biol Sci **323:** 339–355

Lichtenthaler HK (1987) Chlorophylls and carotenoids: pigments of photosynthetic biomembranes. Methods Enzymol **148:** 350–382

Lloyd J, Taylor JA (1994) On the temperature dependence of soil respiration. Funct Ecol **8:** 315–323

Lobell DB, Burke MB, Tebaldi C, Mastrandrea MD, Falcon WP, Naylor RL (2008) Prioritizing climate change adaptation needs for food security in 2030. Science **319:** 607–610

Meinzer F, Plaut Z, Saliendra N (1994) Carbon isotope discrimination, gas exchange and growth of sugarcane cultivars under salinity. Plant Physiol **104:** 521–526

Meinzer F, Saliendra N (1997) Spatial patterns of carbon isotope discrimination and allocation of photosynthetic activity in sugarcane leaves. Aust J Plant Physiol **24:** 769–775

Meinzer F, Zhu J (1998) Nitrogen stress reduces the efficiency of the C_4 CO_2 concentrating mechanism, and therefore quantum yield, in *Saccharum* (sugarcane) species. J Exp Bot **49:** 1227–1234

Mook WG, Bommerson JC, Staverman WH (1974) Carbon isotope fractionations between dissolved bicarbonate and gaseous carbon dioxide. Earth Planet Sci Lett **22:** 169–176

Naidu SL, Moose SP, Al-Shoabi AK, Raines CA, Long SP (2003) Cold-tolerance of C4 photosynthesis in *Miscanthus* x *giganteus*: adaptation in amounts and sequence of C4 photosynthetic enzymes. Plant Physiol **132:** 1–10

O'Leary MH (1988) Carbon isotopes in photosynthesis. Bioscience **38:** 328–336

Osmond CB, Smith FA (1976) Symplastic transport of metabolites during C4 photosynthesis. *In* BES Gunning, AW Robards, eds, Intercellular Communication in Plants: Studies on Plasmodesmata. Springer-Verlag, Berlin, pp 229–241

Reichstein M, Falge E, Baldocchi D, Papale D, Aubinet M, Berbigier P, Bernhofer C, Buchmann N, Gilmanov T, Granier A, et al (2005) On the separation of net ecosystem exchange into assimilation and ecosystem respiration: review and improved algorithm. Glob Change Biol **11:** 1–16

Sage RF (2004) The evolution of C4 photosynthesis. New Phytol **161:** 341–370

Somerville C (2007) Biofuels. Curr Biol **17:** 115–119

Tazoe Y, Hanba YT, Furumoto T, Noguchi K, Terashima I (2008) Relationships between quantum yield for CO_2 assimilation, activity of key enzymes and CO_2 leakiness in *Amaranthus cruentus*, a C4 dicot, grown in high or low light. Plant Cell Physiol **49:** 19–29

Tazoe Y, Noguchi K, Terashima I (2006) Effects of growth light and nitrogen nutrition on the organization of the photosynthetic apparatus in leaves of a C4 plant, *Amaranthus cruentus.* Plant Cell Environ **29:** 691–700

U.S. Department of Energy (2006) Breaking the Biological Barriers to Cellulosic Ethanol: A Joint Research Agenda. DOE/SC-0095. U.S. Department of Energy, Washington, DC, www.doegenomestolife.org/biofuels/

Usuda H (1984) Variations in the photosynthesis rate and activity of photosynthetic enzymes in maize leaf tissue of different ages. Plant Cell Physiol **25:** 1297–1301

Usuda H (1987) Changes in levels of intermediates of the C4 cycle and reductive pentose phosphate pathway under various light intensities in maize leaves. Plant Physiol **84:** 549–554

Villar R, Held AA, Merino J (1995) Dark leaf respiration in light and darkness of an evergreen and a deciduous plant species. Plant Physiol **107:** 412–427

Von Caemmerer S (2000) Modelling C4 photosynthesis. *In* Biochemical Models of Leaf Photosynthesis*:* Techniques in Plant Sciences, 2. CSIRO Publishing, Collingwood, Australia, pp 91–122

Von Caemmerer S, Furbank RT (1999) Modelling C4 photosynthesis. *In* The Biology of C4 Photosynthesis. Physiological Ecology Series. Academic Press, New York, pp 173–211

Von Caemmerer S, Furbank RT (2003) The C4 pathway: an efficient CO_2 pump. Photosynth Res **77:** 191–207

Von Caemmerer S, Ludwig M, Millgate A, Farquhar GD, Price D, Badger M, Furbank RT (1997a) Carbon isotope discrimination during C-4 photosynthesis: insights from transgenic plants. Aust J Plant Physiol **24:** 487–494

Von Caemmerer S, Millgate A, Farquhar GD, Furbank RT (1997b) Reduction of ribulose-1,5-bisphosphate carboxylase/oxygenase by antisense RNA in the C4 plant *Flaveria bidentis* leads to reduced assimilation rates and increased carbon isotope discrimination. Plant Physiol **113:** 469–477

Von Caemmerer S, Quinn V, Hancock NC, Price GD, Furbank RT, Ludwig M (2004) Carbonic anhydrase and C4 photosynthesis: a transgenic analysis. Plant Cell Environ **27:** 697–703

Wang D, Naidu SL, Portis AR Jr, Moose SP, Long SP (2008a) Can the cold-tolerance of C_4 photosynthesis in *Miscanthus* x *giganteus* relative to *Zea mays* be explained by differences in activities and thermal properties of Rubisco? J Exp Bot **59:** 1779–1787

Wang D, Portis AR Jr, Moose SP, Long SP (2008b) Cool C_4 photosynthesis: Pyruvate Pi dikinase expression and activity corresponds to the exceptional cold tolerance of carbon assimilation in Miscanthus × giganteus. Plant Physiol **148:** 557–567